Neurophotonics

Neurophotonics.SPIEDigitalLibrary.org

Coupling of cerebral blood flow and oxygen consumption during hypothermia in newborn piglets as measured by time-resolved near-infrared spectroscopy: a pilot study

Mohammad Fazel Bakhsheshi
Mamadou Diop
Laura B. Morrison
Keith St. Lawrence
Ting-Yim Lee

SPIE.

Coupling of cerebral blood flow and oxygen consumption during hypothermia in newborn piglets as measured by time-resolved near-infrared spectroscopy: a pilot study

Mohammad Fazel Bakhsheshi,[a,b,*] Mamadou Diop,[a,c] Laura B. Morrison,[a] Keith St. Lawrence,[a,b,c] and Ting-Yim Lee[a,b,c,d]
[a]Lawson Health Research Institute, Imaging Program, 268 Grosvenor Street, London, Ontario N6A 4V2, Canada
[b]Robarts Research Institute, Imaging Research Laboratories, 1151 Richmond Street North, London, Ontario N6A 5B7, Canada
[c]Western University, Department of Medical Biophysics, London, Ontario N6A 5C1, Canada
[d]Western University, Department of Medical Imaging, London, Ontario N6A 5W9, Canada

Abstract. Hypothermia (HT) is a potent neuroprotective therapy that is now widely used in following neurological emergencies, such as neonatal asphyxia. An important mechanism of HT-induced neuroprotection is attributed to the associated reduction in the cerebral metabolic rate of oxygen ($CMRO_2$). Since cerebral circulation and metabolism are tightly regulated, reduction in $CMRO_2$ typically results in decreased cerebral blood flow (CBF); it is only under oxidative stress, e.g., hypoxia-ischemia, that oxygen extraction fraction (OEF) deviates from its basal value, which can lead to cerebral dysfunction. As such, it is critical to measure these key physiological parameters during therapeutic HT. This report investigates a noninvasive method of measuring the coupling of $CMRO_2$ and CBF under HT and different anesthetic combinations of propofol/nitrous-oxide (N_2O) that may be used in clinical practice. Both CBF and $CMRO_2$ decreased with decreasing temperature, but the OEF remained unchanged, which indicates a tight coupling of flow and metabolism under different anesthetics and over the mild HT temperature range (38°C to 33°C). [DOI: 10.1117/1.NPh.2.3.035006]

Keywords: brain temperature; indocyanine green; time-resolved near-infrared; cerebral blood flow; cerebral metabolic rate of oxygen; oxygen extraction.

Paper 15028PR received May 27, 2015; accepted for publication Aug. 18, 2015; published online Sep. 21, 2015.

1 Introduction

Mild hypothermia (HT), in which the brain temperature is lowered to 32°C to 33°C, has been shown to be an effective neuroprotective therapy to reduce brain injury following cardiac arrest, traumatic brain injury, birth asphyxia, and ischemic encephalopathy.[1] An important mechanism of HT-induced neuroprotection is the preservation of brain adenosine triphosphate levels resulting from a reduction in the cerebral metabolic rate of oxygen ($CMRO_2$).[2] Indeed, the effects of HT on cerebral blood flow (CBF) are a consequence of the tight coupling between $CMRO_2$ and CBF.[3,4] Preservation of this coupling is an important factor in the control of the cerebral circulation and metabolism, connecting the change in metabolic demands with the supply of substrates by blood flow. As a consequence of this balance between flow and metabolism, the oxygen extraction fraction (OEF) represents a sensitive marker of brain health;[5] under oxidative stress, e.g., hypoxia-ischemia (HI), OEF increases from its basal value of ~33% leading to cerebral venous desaturation.[6–8]

Current methods of measuring cerebral energy metabolism using positron emission tomography and magnetic resonance spectroscopy are not practical for neuromonitoring during prolonged periods of cooling and rewarming phases since therapeutic HT can last up to 72 h.[9,10] By contrast, optical methods are well suited for this since they are safe, compact, portable, and can provide continuous monitoring at the bedside. We have previously developed a dynamic contrast-enhanced near-infrared spectroscopy (NIRS) technique for measuring absolute CBF and $CMRO_2$ using the light-absorbing dye, indocyanine green (ICG), as an intravascular contrast agent in newborn piglets[11–15] and adult porcine model.[16–18] However, there has been no previous study investigating the feasibility of using time-resolved (TR) NIRS to measure CBF and $CMRO_2$ during HT.

Although the results from a recent study have shown that neonates with hypoxic-ischemic encephalopathy have lower blood flow index and relative $CMRO_2$ during cooling when compared to healthy neonates,[19] the effect of HT on flow-metabolism coupling under different anesthetic regimes on the noninjured brain has not been studied to our knowledge. In the present study, CBF and $CMRO_2$ were measured by TR-NIRS in healthy newborn piglets under isoflurane for induction of anesthesia and then both measurements were repeated under propofol/nitrous oxide (N_2O) while the brain temperature was lowered from ~38°C to 33°C.

*Address all correspondence to: Mohammad Fazel Bakhsheshi, E-mail: mfazelba@alumni.uwo.ca

2329-423X/2015/$25.00 © 2015 SPIE

2 Materials and Methods

2.1 *Instrumentation*

The light sources of the time-resolved system were thermoelectrically cooled picosecond pulsed diode lasers (LDH-P-C emitting at 760, 810, and 830 nm, PicoQuant, Germany) activated by a computer-controlled laser driver (SEPIA PDL 828, PicoQuant). The 760- and 830-nm emission wavelengths were chosen to quantify tissue oxyhemoglobin (HbO_2) and deoxyhemoglobin (Hb) concentrations, which were used to determine the cerebral oxygen saturation, whereas the 810-nm laser coincides with the peak absorption wavelength of ICG in plasma. The output power and pulse repetition rates of the lasers were set to 1.4 mW and ~27 MHz, respectively. The individual pulses of the lasers were temporally separated by sharing the 80-MHz clock of the laser driver among the three lasers. Light emitted by each diode laser was attenuated by two adjustable neutral density filters (NDC-50-4M, Thorlabs, Newton, New Jersey) and coupled by a microscope objective lens (NA = 0.25, magnification = 10×) into one arm of a trifurcated fiber bundle (three step-index multimode fibers, NA = 0.22, core 400 μm; Fiber Optics Technology, Pomfret, Connecticut). The distal common end of the bundle (emission probe) was placed on the scalp of the animal and held in position by a probe holder. The average power delivered to a subject was attenuated to ~20 μW/laser, which is below ANSI safety limits for skin exposure.[20]

Photons emerging from the scalp were collected by another fiber bundle (multimode step-index fibers, NA = 0.55, 3.6 mm diameter active area; Fiber Optics Technology, Pomfret, Connecticut). The other end of the fiber bundle was secured in front of an electromechanical shutter (SM05, Thorlabs). Light transmitted through the shutter was collected by a Peltier cooled microchannel plate photomultiplier tube (PMC-100, Becker and Hickl, Germany). Detection of single photons generated electrical pulses (amplitude of 50 to 200 mV, width = 1.5 ns) that were transmitted to a time-correlated single-photon counting (TCSPC) module (SPC-134, Becker and Hickl) to generate the temporal point spread function (TPSF). The TCSPC module had a dead time of 100 ns, and because of that, the maximum count rate per laser was constrained to ~800 kHz (i.e., one photon detected every 1.25 μs) to minimize dead-time effects. This count rate, which was ~3% of the laser pulse repetition rate, also minimized pileup effects.[21]

2.2 *Optical Properties Measurement*

To quantify tissue optical properties from the measured TPSFs, the instrument response function (IRF) was measured to account for the temporal dispersion in the system.[22] IRFs were measured at the start and end of each experiment at the same count rate as the TPSFs (800 kHz). Figure 1 shows a typical IRF of the TR instrument (FWHM = 390 ps) and a TPSF measured on a piglet's head at a source-detector distance of 20 mm. Both TPSFs and IRF were acquired at 800 kHz at a sampling interval of 400 ms. The tissue optical properties were obtained using an analytical model of light diffusion.[23] The model solution was first convolved with the measured IRF, and a nonlinear optimization routine (based on the MATLAB® function *fminsearch*) was used to fit the convolved model to each measured TPSF to determine the absorption coefficient (μ_a), reduced scattering coefficient (μ_s'), and a scaling factor, which accounts for variations in laser power, detection gain, and coupling efficiency.[22] The fitting range was set to 80% prior to the peak of the TPSF, as diffusion modeling is known to be a poor model for early photons[24,25] and 20% after the peak to minimize the effects of noise. Tissue optical properties at each temperature were determined by averaging 32 TPSFs collected over 320 s. For the hemodynamics measurements, changes in light absorption caused by ICG were characterized using only μ_a as a fitting parameter, with μ_s' and the scaling factor was fixed to their baseline values. Finally, the measured change in the absorption coefficient was used to compute the ICG concentration, as discussed in the following section.

2.3 *Determination of Cerebral Blood Flow*

CBF was quantified using a bolus-tracking method that requires an intravenous bolus injection of ICG (1 ml, 0.2 mg/kg) into a peripheral vein, followed by continuous measurement of the time-varying concentration of the dye in arterial blood and brain tissue. The arterial concentration, $C_a(t)$, was measured noninvasively by a dye densitometer (model DDG-2001 A/K, Nihon Kohden, Tokyo, Japan) with the probe attached to a front foot of the animal. Brain tissue concentration of ICG, $C_{tis}(t)$, was determined from the measured changes in μ_a acquired continuously for 76 s at a sampling interval of 400 ms:[12]

$$C_{tis}(t) = [\mu_a(t) - \mu_a(0)]/[\ln(10) \times \varepsilon_{ICG}], \quad (1)$$

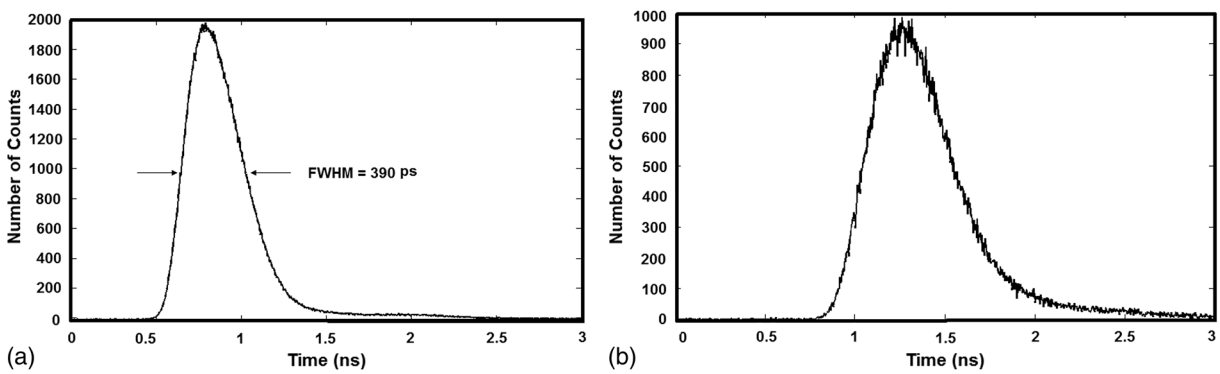

Fig. 1 (a) Typical instrument response function of the time-resolved (TR) instrument with a FWHM of 390 ps and (b) a temporal point spread function acquired at the same wavelength on the piglet head at a source-detector distance of 20 mm.

where $\mu_a(0)$ represents the baseline absorption coefficient determined over a 10-s period prior to ICG injection and ε_{ICG} is the extinction coefficient of ICG at 802 nm (186 OD/mM/cm).[26] The brain (tissue) and arterial concentrations of ICG are related by the following equation:

$$C_{tis}(t) = C_a(t) * [\mathrm{CBF} \cdot R(t)], \tag{2}$$

where * represents the convolution operator and $\mathrm{CBF} \cdot R(t)$ is the flow-scaled impulse residue function, i.e., $R(t)$ scaled by CBF. The function $\mathrm{CBF} \cdot R(t)$ was extracted from the arterial and tissue ICG concentration curves [i.e., Eq. (2)] using a deconvolution algorithm.[27] The initial height of the derived function is CBF, since by definition $R(0) = 1$.[28] Figure 2 shows typical brain and arterial ICG concentration curves measured with the TR-NIRS technique and a pulse dye densitometer under isoflurane at 38°C. The peak arterial concentration is ~20 to 30 times greater than that of tissue concentration since the cerebral blood volume (CBV) is about 3% to 5% of the total brain volume.

2.4 *Determination of Cerebral Oxygen Metabolism and Extraction Fraction*

$\mathrm{CMRO_2}$ was calculated using Fick's principle:[11]

$$\mathrm{CMRO_2} = \mathrm{CBF}([\mathrm{O_2}]_a - [\mathrm{O_2}]_v). \tag{3}$$

The difference between the arterial oxygen concentration, $[\mathrm{O_2}]_a$, and the cerebral venous concentration of oxygen, $[\mathrm{O_2}]_v$, is commonly referred to as the arteriovenous oxygen difference and is the difference between the $\mathrm{O_2}$ concentration of the arterial blood feeding the tissue of interest and $\mathrm{O_2}$ concentration of the venous blood draining the tissue. Equation (3) can be further expanded as follows:[29]

$$\mathrm{CMRO_2} = \mathrm{CBF}\, 1.39\, [\mathrm{tHb}]\, (S_a\mathrm{O_2} - S_v\mathrm{O_2}), \tag{4}$$

where [tHb] is total hemoglobin concentration, which can be measured from blood samples. $S_a\mathrm{O_2}$ and $S_v\mathrm{O_2}$ are arterial and venous $\mathrm{O_2}$ saturation, respectively. The constant 1.39 is the $\mathrm{O_2}$ carrying capacity of hemoglobin measured in milliliters per gram of Hb. Note that the dye densitometer also provides continuous measurements of $S_a\mathrm{O_2}$, whereas $S_v\mathrm{O_2}$ was determined indirectly from the TR-NIRS measurements of the cerebral blood oxygen saturation, $S_{tis}\mathrm{O_2}$. This technique relies on the assumption that there exists a stable arterial-venous blood ratio in the CBV:[30,31]

$$S_{tis}\mathrm{O_2} = \alpha S_a\mathrm{O_2} + (1-\alpha) S_v\mathrm{O_2}, \tag{5}$$

where α represents the fraction of arterial blood in CBV. The relative distribution of arterial and venous compartments is generally accepted to be ~25% and 75% of the total CBV; therefore, α was set to 0.25.[30,31] To obtain tissue cerebral blood oxygen saturation, i.e., $S_{tis}\mathrm{O_2}$, cerebral hemoglobin ($\mathrm{HbO_2}$, Hb) concentrations were calculated from the TR-NIRS measurements. These hemoglobin concentrations were determined by fitting the tissue absorption coefficients to the extinction coefficients of Hb and $\mathrm{HbO_2}$, assuming a stable concentration of 85% water in the brain.[32] A least-square optimization algorithm (MATLAB function *fminsearch*) was used to extract the concentrations of oxy- and deoxyhemoglobin from the absorption coefficients measured at the three wavelengths. $S_{tis}\mathrm{O_2}$ was then calculated as follows:

$$S_{tis}\mathrm{O_2} = \frac{\mathrm{HbO_2}}{\mathrm{HbO_2} + \mathrm{Hb}}. \tag{6}$$

Using this relationship, a new expression for $\mathrm{CMRO_2}$ can be derived that is independent of $S_v\mathrm{O_2}$:

$$\mathrm{CMRO_2} = \mathrm{CBF}\, 1.39\, [\mathrm{tHb}] \left(\frac{S_a\mathrm{O_2} - S_{tis}\mathrm{O_2}}{1-\alpha}\right). \tag{7}$$

The fraction of oxygen extracted from arterial blood into the brain, OEF, was also calculated using the method described by Brown et al.:[11]

$$\mathrm{OEF} = \frac{\mathrm{CMRO_2}}{\mathrm{CBF}[\mathrm{O_2}]_a}. \tag{8}$$

The tight coupling of CBF and $\mathrm{CMRO_2}$ in the normal brain leads to a stable level of OEF around ~33%.[33] A decoupling

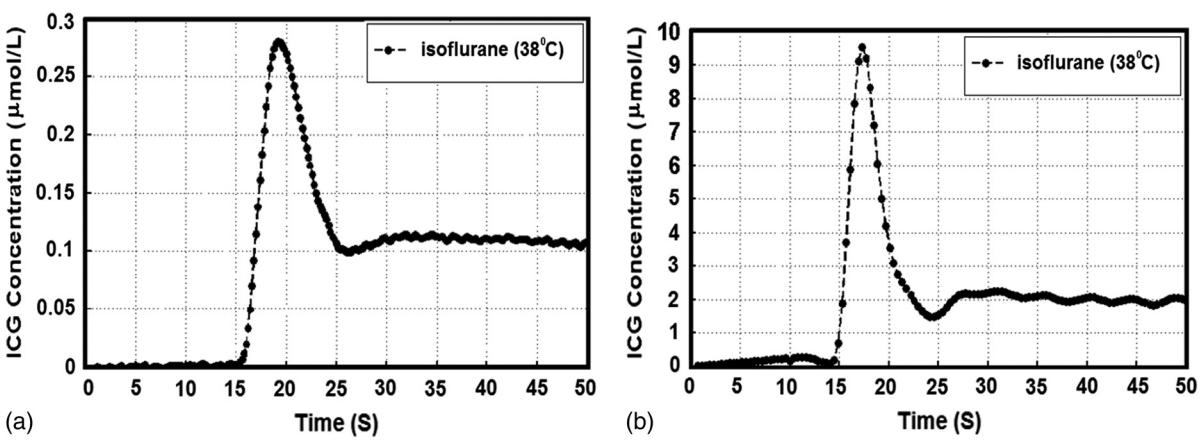

Fig. 2 Samples (a) tissue ICG concentration curve measured with the TR near-infrared spectroscopy (NIRS) technique and (b) arterial ICG concentration curve obtained with the pulse dye densitometer from indocyanine green (ICG) bolus injection under isoflurane at brain temperature of 38°C. Both tissue and arterial curves were measured simultaneously over a period of 50 s during injection of 1.0 ml of ICG solution at a concentration of 0.1 mg/ml.

of the two signifies oxidative stress and can lead to an increase in OEF beyond the normal value.[7]

2.5 *Animal Preparation and Experimental Procedure*

Experiments were conducted on five newborn piglets. All animal experiments were approved by the Animal Use Subcommittee of the Canadian Council on Animal Care at our institution. Newborn Duroc cross piglets were obtained from a local supplier on the morning of the experiment. Anesthesia was induced with 1% to 2% isoflurane, which was increased to 3% to 4% during preparatory surgery. A tracheotomy was performed and the piglet was ventilated with oxygen and medical air mixture. A femoral artery was catheterized to monitor heart rate (HR) and mean arterial blood pressure (MAP) and to intermittently collect arterial blood samples for gas (p_aCO_2, p_aO_2), pH, and glucose concentration analysis. A cannula was inserted into an ear vein for infusion of propofol (AstraZeneca Pharmaceuticals, Inc., Canada) and ICG injection (Sigma-Aldrich, Saint Louis, Missouri). After surgery, piglets were maintained on 1% to 2% isoflurane at normothermia ($NT_{38°C}$). Arterial CO_2 tension (p_aCO_2) was monitored throughout the experiment, either directly by blood gas measurements or by the end-tidal CO_2 tension, and maintained at normocapnia between 37 and 40 mmHg by adjusting the breathing rate and ventilation volume. Arterial oxygen tension (p_aO_2) was maintained at a level between 90 and 130 mmHg by adjusting the ratio of oxygen to medical air. Blood glucose was monitored intermittently and if it fell below 4.5 mmol/l, then a 1 to 2 ml infusion of 25% dextrose solution was administered intravenously. Brain temperature was also measured with a thermocouple probe. The needle thermocouple probe was inserted laterally into the brain to a depth of 2 cm vertical from the brain surface and 0.5 cm posterior to the bregma. Animals were placed in the prone position and a custom-made probe holder was strapped to the head to hold the TR-NIRS emission and detection probes 2 cm apart, parasagittally, ~1.5 cm dorsal to the eyes. Figure 3 shows a schematic of a piglet's head with the locations of the emission and detection probes as well as the needle thermocouple. The experiments started after a delay of 60 min to allow time for the animal to stabilize following surgery. This delay was also sufficient for the TR instrument to reach a quasiequilibrium to minimize drift artifacts induced by temperature fluctuations in the TR-NIRS instrument.[34]

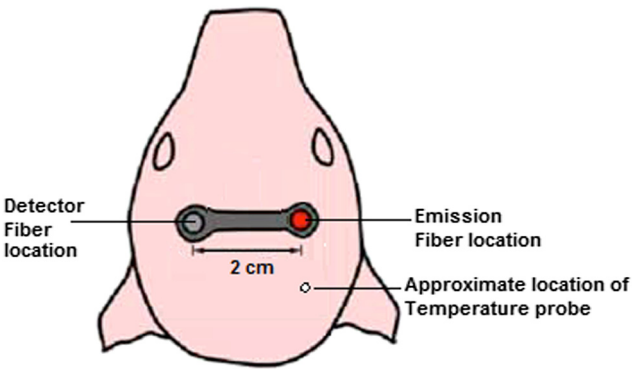

Fig. 3 Schematic of a piglet head showing the location of the detection, emission probes, and approximate position of the needle thermocouple probe to measure brain temperature. The emission-detector distance was 2 cm.

After the stabilization period, CBF and $CMRO_2$ were first measured under isoflurane (1% to 2%) and then under intravenous infusion of propofol (9 to 22.4 mg/kg/h) and ventilation with 70% nitrous oxide ($N_2O_{70\%}$) and 30% oxygen ($O_{2\ 30\%}$) while brain temperature was lowered from normothermia (38°C) to HT (35° and 33°C). For propofol (10 mg/ml) infusion, the rate was adjusted according to the animal's response to pain stimuli and change in vital signs such as blood pressure and HR with a mean infusion rate of 2.51 ± 1.15 ml/h. For normothermia, a heated water blanket was used to maintain rectal and brain temperature between 38°C to 38.5°C. HT was induced by placing plastic ice bags on the surface of the piglet's body. Each experiment was completed within 5 h and after the last measurement, the animal was euthanized with intravenous potassium chloride (1 to 2 ml/kg, 2 mEq/ml) infusion. The time-limiting factor of the proposed CBF method is the necessity for ICG to be cleared from the blood stream by the liver. Since that takes about 10 to 15 min, CBF measurement can only be acquired every 15 min. Figure 4 illustrates the experimental workflow; tissue oxygen saturation (S_{tis}) and CBF were acquired in two blocks during each condition. All data sets for each condition were acquired within ~15 min.

2.6 *Statistical Analysis*

SPSS 17.0.0 (SPSS, Inc, Chicago, Illinois) was used for all statistical analyses. Wilcoxon test was used to determine statistical differences between measurements acquired under normothermia (38°C) when the anesthetic was switched from isoflurane to propofol/N_2O. Comparisons between temperature-based measurements were performed using the Friedman test. Statistical significance was based on p-value <0.05. All data are presented as mean ± standard deviation unless otherwise noted.

3 Results

Experiments were conducted on five piglets (three females and two males), with an average age of 34 ± 6 h and an average weight of 1.4 ± 0.3 kg. Table 1 presents a summary of the physiological parameters (MAP, HR, p_aCO_2, p_aO_2, pH, S_aO_2, $[O_2]_a$ and $S_{tis}O_2$) for the different anesthetic groups and brain temperatures. When the anesthetic was switched from isoflurane (baseline) to propofol/N_2O, there were statistically significant increases in HR and MAP ($p < 0.05$) compared to baseline; however, HR started to decrease immediately after initiation of cooling. Additionally, a statistically significant ($p < 0.05$) decrease in p_aO_2 was observed when the temperature fell below 35°C. There were no significant changes in p_aCO_2, S_aO_2, $[O_2]_a$, tHb, pH, and $S_{tis}O_2$ with temperature.

Figure 5(a) displays CBF and $CMRO_2$ measurements under isoflurane at normothermia (38°C) and under propofol/N_2O mixture at three different brain temperatures. At normothermia, both CBF and $CMRO_2$ decreased from 50.4 ± 13.1 to 31.3 ± 8.8 ml min^{-1} 100 g^{-1} and 2.4 ± 0.6 to 1.5 ± 0.4 mlO_2 min^{-1} 100 g^{-1}, respectively, when the anesthetic was switched from isoflurane to propofol/N_2O. There was also a progressive reduction in CBF from 31.3 ± 8.8 to 24.1 ± 5.9 ml min^{-1} 100 g^{-1} and $CMRO_2$ from 1.5 ± 0.4 to 1.1 ± 0.1 mlO_2 min^{-1} 100 g^{-1} when brain temperature decreased from 38°C to 33°C under propofol/N_2O. The OEF values under the different anesthetics and brain temperatures are displayed in Fig. 5(b). It shows that OEF did not deviate from its basal value under the different anesthetic and

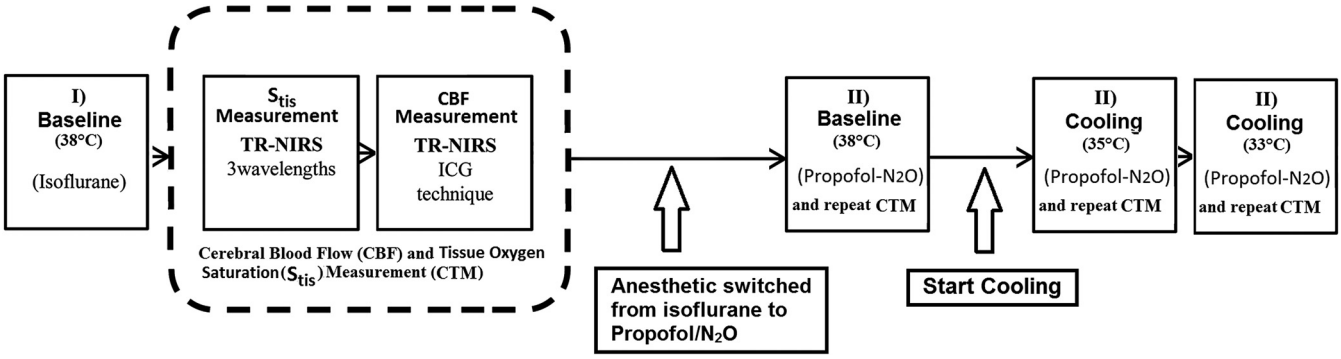

Fig. 4 Experimental workflow: the solid boxes are distinctive steps, whereas the dotted box is recurring for each induced condition.

Table 1 Physiological parameters measured at different brain temperatures. S_aO_2, oxygen saturation of arterial blood; p_aO_2, partial pressure of oxygen in arterial blood; MAP, mean arterial pressure; HR, heart rate; tHb, total hemoglobin concentration in arterial blood; p_aCO_2, partial pressure of carbon dioxide in arterial blood; $[O_2]_a$, arterial concentration of oxygen; $S_{tis}O_2$, tissue cerebral blood oxygen saturation;

Variable		Baseline (isoflurane)	Cooling (propofol-N_2O)		
		(38°C)	(38°C)	(35°C)	(33°C)
	Baseline/Cooling				
MAP (mmHg)	(Isoflurane/propofol-N_2O)	42 ± 4	$56 \pm 6^*$	$52 \pm 2^*$	$50 \pm 11^*$
HR (bpm)	(Isoflurane/propofol-N_2O)	148 ± 5	$226 \pm 41^*$	$195 \pm 8^*$	138 ± 28
p_aCO_2 (mmHg)	(Isoflurane/propofol-N_2O)	40 ± 2	41 ± 2	41 ± 1	40 ± 2
p_aO_2 (mmHg)	(Isoflurane/propofol-N_2O)	155 ± 40	210 ± 49	$136 \pm 4^*$	$85 \pm 16^*$
pH	(Isoflurane/propofol-N_2O)	7.4 ± 0.1	7.4 ± 0.1	7.3 ± 0.1	7.3 ± 0.1
tHb (μmol/l)	(Isoflurane/propofol-N_2O)	8.1 ± 0.3	8.3 ± 0.8	8.5 ± 1.1	8.4 ± 1.2
S_aO_2 (%)	(Isoflurane/propofol-N_2O)	100	97 ± 2	98 ± 1	97 ± 1
$[O_2]_a$ (ml/dl)	(Isoflurane/propofol-N_2O)	11 ± 1	11 ± 2	11 ± 2	11 ± 1
$S_{tis}O_2$ (%)	(Isoflurane/propofol-N_2O)	0.69 ± 0.01	0.69 ± 0.01	0.69 ± 0.01	0.69 ± 0.01

*A statistically significant ($p < 0.05$) difference compared to the baseline.

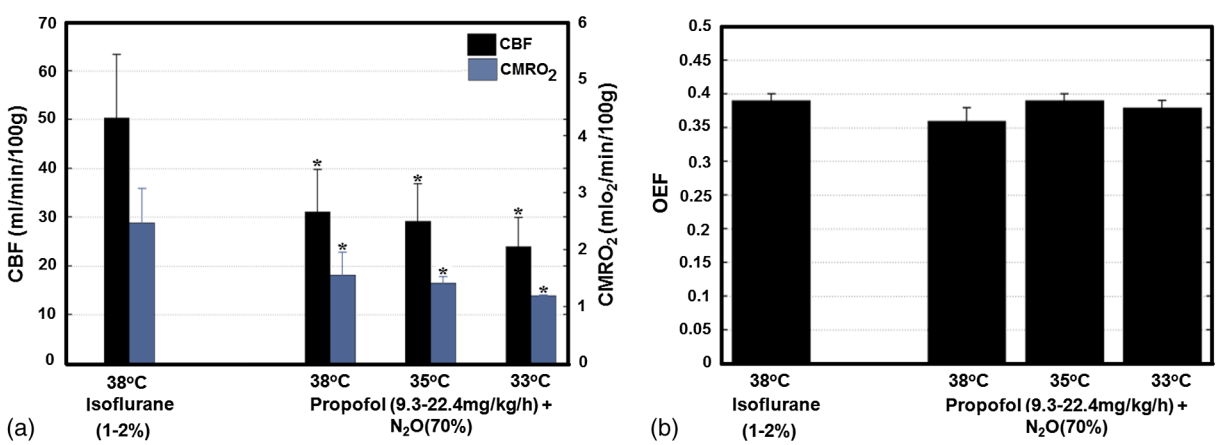

Fig. 5 (a) Cerebral blood flow (CBF) and oxygen metabolic rate ($CMRO_2$); and (b) oxygen extraction fraction (OEF) at each brain temperature under isoflurane or propofol/N_2O anesthesia ($N = 5$). Values are shown as mean ± SD; *$p < 0.05$ versus at 38°C with isoflurane (baseline).

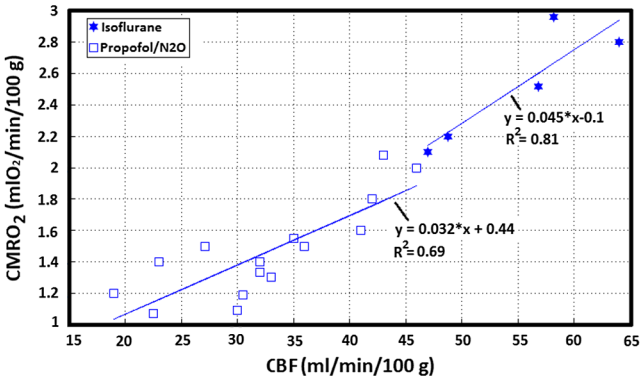

Fig. 6 Plot of CBF and $CMRO_2$ during cooling under different anesthetic conditions. Each symbol type represents data for each anesthetic group. The lines indicate the line of regression associated with each group.

temperature combinations, confirming the tight coupling between CBF and $CMRO_2$; any change in metabolic demand was met by a corresponding change in substrate delivery via CBF modulation.

Figure 6 shows the relationships between $CMRO_2$ and CBF under the different anesthetic groups at baseline and during HT; there is a strong linear dependence of CBF on $CMRO_2$ for both anesthetic groups. This result shows that brain temperatures and anesthetics did not alter the CBF and $CMRO_2$ coupling in the healthy brain; however, this might not be the case for an injured brain.

4 Discussion

We investigated the relationship between $CMRO_2$ and CBF under normothermia (38°C) and mild whole body HT (35°C or 33°C) with two different anesthetics, isoflurane (1% to 2%)/($N_{2\ 66\%}$, $O_{2\ 33\%}$), and propofol/($N_2O_{70\%}$, $O_{2\ 30\%}$), which is representative of what may be used in clinical practice.[35] Previous studies have shown that the temperature range associated with better neurological outcomes is between 33°C and 35°C.[36] However, cooling the whole body below 34°C can induce severe complications including shivering, skin erythema, renal failure, coagulopathy, pulmonary hypertension, reducing cardiac, and increased mortality.[37,38] Consequently, to limit the deleterious effects of whole body cooling, only mild HT, in which the brain temperature is decreased to 33°C, has been applied in this study. Our results showed that compared to normothermia, mild HT decreases both CBF and $CMRO_2$ with preserved flow-metabolism coupling shown by constant OEF under different anesthetics. Flow-metabolism coupling within the brain is a complex physiologic process that is regulated by a combination of metabolic, glial, neural, and vascular factors.[5,39,40] In the normal brain, autoregulated CBF is cerebrovascular and metabolic reactivity induced by changes in arterial carbon dioxide tension operate to maintain a tight coupling between CBF and $CMRO_2$. However, during cerebral ischemic insults, alterations of cerebral hemodynamic and metabolism are highly dynamic. As cerebral perfusion pressure (CPP) falls, CBF is maintained by autoregulation[41] through vasodilatation of resistance arterioles, but when the capacity for compensatory vasodilation is exceeded, autoregulation fails and CBF falls as a function of CPP. When oxygen supply is diminished due to decreasing CBF, OEF increases in an effort to compensate for the reduced CBF to maintain $CMRO_2$ commensurate with metabolic demand and preserve neuronal function and cellular integrity.[5] If CPP continues to fall, CBF will progressively decline until the increase in OEF is no longer sufficient to supply the necessary oxygen to meet metabolic demand; energy failure will result and permanent tissue damage follows. Therefore, increased OEF from its basal value may be a sensitive and specific marker of oxidative stress that can lead to cerebral dysfunction.

The vasodilating effects of isoflurane have limited its use as a sedative agent in the neurosurgical intensive care unit (NICU) because of the fear of a potential increase in intracranial pressure (ICP) caused by the increase in CBF.[42] By contrast, propofol is being used more frequently in the NICU, particularly for head-injury cases.[43] Propofol is known to decrease CBF while preserving brain flow-metabolism coupling and acts as a global central nervous system depressant.[42] It has been shown that a typical anesthetic induction dose of propofol reduces blood pressure by ~30% resulting from a decrease in sympathetic activity, direct vasodilation, and myocardial depression.[44,45] When the anesthetic was switched from isoflurane to propofol, there was a statistically significant increase in HR, suggesting that decrease in peripheral vascular resistance induced by propofol was partially compensated by an increase in HR.[42]

In the present study, TR-NIRS was used to separate the effects of tissue scattering from absorption and measure both endogenous and exogenous tissue chromophore concentrations.[46] Although quantitative and mobile, a limitation with the TR-NIR technique is the need to inject a bolus of ICG every time CBF is measured. However, this is a minimally invasive procedure since ICG is injected into a peripheral vein and the time-dependent arterial ICG concentration curve can be measured noninvasively by pulse dye densitometry. Furthermore, ICG is approved for clinical use in North America and the incidence of allergic reactions to the dye is very low (~1:250,000) in both adults and newborns.[47] Recently, Verdecchia et al. have shown that TR-NIRS can be combined with diffuse correlation spectroscopy to provide a quasicontinuous quantitative assessment of CBF and $CMRO_2$.[14] With this approach, only infrequent injections of ICG are needed to calibrate the continuous measurement of changes in CBF and $CMRO_2$ into absolute values.

The superficial layer on the newborn head (scalp and skull) is relatively thin (about 1 to 2 mm) so that the contribution of the extracerebral tissue layer to the signal is relatively small. Consequently, the TPSFs were analyzed using the solution to the diffusion equation for a semi-infinite homogeneous medium.[12] Extracerebral contamination is a major issue in the adult studies because of the greater thickness of the scalp and skull;[16] however, depth-resolved approaches enable the separation superficial contributions and deep components on the basis that light penetration increases with source-detector distance. Furthermore, TR-NIRS has the ability to distinguish early from late arriving photons. Since photons with extended time-of-flight have a higher probability of probing deeper tissue, TR-NIRS can discriminate superficial from deep tissue absorption from measurements acquired at a single source-detector.[48]

A potential concern with our experimental procedure is that anesthesia was initiated with isoflurane during preparatory surgery and at normothermia. Besides being an easy to use anesthetic agent to induce anesthesia, isoflurane increases CBF relative to propofol/nitrous oxide and affords the condition to investigate whether autoregulation responses (flow metabolism coupling) remain intact at low-dose isoflurane at

normothermia.[49] Understanding how the combination of HT under different anesthetics may alter flow-metabolism coupling or OEF from its basal values in the healthy brain is critical before extending these neuroprotective strategies to the injured brain. Therefore, it might be worth trying different anesthetic induction agents in future studies. As well, rewarming is a critical phase of therapeutic HT in which too fast rewarming rates may retrigger destructive processes at the cellular level.[50] Rapid rewarming of the injured brain commonly leads to a mismatch between cerebral metabolism and perfusion (hence increased OEF) and can cause rebound ICP elevations, cerebral venous desaturation, and brain ischemia. It is suggested that controlling the rewarming rate to as low as 0.1°C to 0.4°C/h is preferred to reduce the neurological risks.[51] Therefore, monitoring for possible deleterious effects of rewarming via TR-NIRS measurement of OEF as developed in this study is important for guaranteeing HT treatment efficacy.

5 Conclusion

We have measured the cerebral metabolic activity ($CMRO_2$) and CBF at different temperatures in a neonatal animal model. Both CBF and $CMRO_2$ decreased with lowering of the brain temperature but the OEF remained unchanged, which indicates a tight coupling of flow and metabolism over the mild HT temperature range (38°C to 33°C). This tight coupling might not be preserved leading to increased OEF above the normal values when oxidative stress occurs as in the ischemic brain. Furthermore, rewarming is a critical phase of therapeutic HT to monitor for oxidative stress.[10,52] Rapid rewarming of the injured brain commonly leads to a mismatch between cerebral metabolism and perfusion[10] (hence increased OEF) and can cause rebound ICP elevations,[53] cerebral venous desaturation,[52] and brain ischemia. It is suggested that controlling the rewarming rate to as low as 0.1°C to 0.4°C/h is preferred to reduce the neurological risks.[54] Therefore, monitoring for possible deleterious effects of rewarming via TR-NIRS measurement of OEF as developed in this study is important for guaranteeing HT treatment efficacy. Although the results from this pilot study were encouraging, more animal experiments will be required to evaluate flow-metabolism coupling in the injured brain, e.g., in HI.

Acknowledgments

The authors would like to thank Jennifer Hadway for her help in conducting the animal experiments. This study was funded in part through support from the Canadian Institutes of Health Research and the Heart and Stroke Foundation of Canada.

References

1. E. M. Moore et al., "Therapeutic hypothermia: benefits, mechanisms and potential clinical applications in neurological, cardiac and kidney injury," *Injury* **42**, 843–854 (2011).
2. M. Erecinska et al., "Effects of hypothermia on energy metabolism in mammalian central nervous system," *J. Cereb. Blood Flow Metab.* **23**, 513–530 (2003).
3. M. Sakoh and A. Gjedde, "Neuroprotection in hypothermia linked to redistribution of oxygen in brain," *Am. J. Physiol. Heart Circ. Physiol.* **285**, H17–H25 (2003).
4. M. P. Ehrlich et al., "Effect of hypothermia on cerebral blood flow and metabolism in the pig," *Ann. Thorac. Surg.* **73**, 191–197 (2002).
5. W. J. Powers et al., "Cerebral blood flow and cerebral metabolic rate of oxygen requirements for cerebral function and viability in humans," *J. Cereb. Blood Flow Metab.* **5**, 600–608 (1985).
6. G. Q. Cheng et al., "Effects of selective head cooling on cerebral blood flow and cerebral metabolic rate in newborn piglets," *Zhonghua Er Ke Za Zhi* **43**, 748–752 (2005).
7. W. J. Powers, "Cerebral hemodynamics in ischemic cerebrovascular disease," *Ann. Neurol.* **29**, 231–240 (1991).
8. C. P. Derdeyn et al., "Variability of cerebral blood volume and oxygen extraction: stages of cerebral haemodynamic impairment revisited," *Brain* **125**, 595–607 (2002).
9. D. Azzopardi et al., "Treatment of asphyxiated newborns with moderate hypothermia in routine clinical practice: how cooling is managed in the UK outside a clinical trial," *Arch. Dis. Child Fetal Neonatal Ed.* **94**, F260–F264 (2009).
10. S. Enomoto et al., "Rapid rewarming causes an increase in the cerebral metabolic rate for oxygen that is temporarily unmatched by cerebral blood flow. A study during cardiopulmonary bypass in rabbits," *Anesthesiology* **84**, 1392–1400 (1996).
11. D. W. Brown et al., "Near-infrared spectroscopy measurement of oxygen extraction fraction and cerebral metabolic rate of oxygen in newborn piglets," *Pediatr. Res.* **54**, 861–867 (2003).
12. M. Diop et al., "Comparison of time-resolved and continuous-wave near-infrared techniques for measuring cerebral blood flow in piglets," *J. Biomed. Opt.* **15**, 057004 (2010).
13. D. W. Brown et al., "Quantitative near infrared spectroscopy measurement of cerebral hemodynamics in newborn piglets," *Pediatr. Res.* **51**, 564–570 (2002).
14. K. Verdecchia et al., "Quantifying the cerebral metabolic rate of oxygen by combining diffuse correlation spectroscopy and time-resolved near-infrared spectroscopy," *J. Biomed. Opt.* **18**, 027007 (2013).
15. K. M. Tichauer et al., "Measurement of cerebral oxidative metabolism with near-infrared spectroscopy: a validation study," *J. Cereb. Blood Flow Metab.* **26**, 722–730 (2006).
16. J. T. Elliott et al., "Quantitative measurement of cerebral blood flow in a juvenile porcine model by depth-resolved near-infrared spectroscopy," *J. Biomed. Opt.* **15**, 037014 (2010).
17. J. T. Elliott et al., "Quantifying cerebral blood flow in an adult pig ischemia model by a depth-resolved dynamic contrast-enhanced optical method," *Neuroimage* **94**, 303–311 (2014).
18. J. T. Elliott et al., "Variance of time-of-flight distribution is sensitive to cerebral blood flow as demonstrated by ICG bolus-tracking measurements in adult pigs," *Biomed. Opt. Express* **4**, 206–218 (2013).
19. M. Dehaes et al., "Cerebral oxygen metabolism in neonatal hypoxic ischemic encephalopathy during and after therapeutic hypothermia," *J. Cereb. Blood Flow Metab.* **34**, 87–94 (2013).
20. R. H. Ossoff, "Implementing the ANSI Z 136.3 laser safety standard in the medical environment," *Otolaryngol. Head Neck Surg.* **94**, 525–528 (1986).
21. W. Becker, *Advanced Time-Correlated Single Photon Counting Technique*, Springer, New York (2005).
22. V. Ntziachristos and B. Chance, "Accuracy limits in the determination of absolute optical properties using time-resolved NIR spectroscopy," *Med. Phys.* **28**, 1115–1124 (2001).
23. A. Kienle and M. S. Patterson, "Improved solutions of the steady-state and the time-resolved diffusion equations for reflectance from a semi-infinite turbid medium," *J. Opt. Soc. Am. A Opt. Image Sci. Vis.* **14**, 246–254 (1997).
24. K. M. Yoo et al., "When does the diffusion approximation fail to describe photon transport in random media?," *Phys. Rev. Lett.* **64**, 2647–2650 (1990).
25. R. Cubeddu et al., "Experimental test of theoretical models for time-resolved reflectance," *Med. Phys.* **23**, 1625–1633 (1996).
26. M. L. Landsman et al., "Light-absorbing properties, stability, and spectral stabilization of indocyanine green," *J. Appl. Physiol.* **40**, 575–583 (1976).
27. A. Cenic et al., "Dynamic CT measurement of cerebral blood flow: a validation study," *AJNR Am. J. Neuroradiol.* **20**, 63–73 (1999).
28. K. L. Zierler, "Equations for measuring blood flow by external monitoring of radioisotopes," *Circ. Res.* **16**, 309–321 (1965).
29. N. Roche-Labarbe et al., "Noninvasive optical measures of CBV, StO (2), CBF index, and rCMRO(2) in human premature neonates' brains in the first six weeks of life," *Hum. Brain Mapp.* **31**, 341–352 (2010).
30. G. Mchedlishvili, *Arterial Behavior and Blood Circulation in the Brain*, Consultants Bureau, New York (1986).

31. H. M. Watzman et al., "Arterial and venous contributions to near-infrared cerebral oximetry," *Anesthesiology* **93**, 947–953 (2000).
32. D. R. White et al., "The composition of body tissues (II). Fetus to young adult," *Br. J. Radiol.* **64**, 149–159 (1991).
33. A. Nozari et al., "Maximisation of cerebral blood flow during experimental cardiopulmonary resuscitation does not ameliorate post-resuscitation hypoperfusion," *Resuscitation* **40**, 27–35 (1999).
34. M. Diop et al., "Time-resolved near-infrared technique for bedside monitoring of absolute cerebral blood flow," *Proc. SPIE* **7555**, 75550Z (2010).
35. C. Yokoe et al., "The effect of nitrous oxide inhalation on the hypotensive response to propofol: a randomized controlled trial," *Oral Surg. Oral Med. Oral Pathol. Oral Radiol.* **118**, 166–173 (2013).
36. P. J. Andrews et al., "European society of intensive care medicine study of therapeutic hypothermia (32–35 degrees C) for intracranial pressure reduction after traumatic brain injury (the Eurotherm3235Trial)," *Trials* **12**, 8 (2011).
37. M. Okada, "The cardiac rhythm in accidental hypothermia," *J. Electrocardiol.* **17**, 123–128 (1984).
38. R. Y. Chen and S. Chien, "Hemodynamic functions and blood viscosity in surface hypothermia," *Am. J. Physiol.* **235**, 136–143 (1978).
39. D. Attwell et al., "Glial and neuronal control of brain blood flow," *Nature* **468**, 232–243 (2010).
40. E. C. Peterson et al., "Regulation of cerebral blood flow," *Int. J. Vasc. Med.* **2011**, 823525 (2011).
41. E. T. MacKenzie et al., "Effects of hemorrhagic hypotension on the cerebral circulation. I. Cerebral blood flow and pial arteriolar caliber," *Stroke* **10**, 711–718 (1979).
42. F. Villa et al., "Inhalation versus endovenous sedation in subarachnoid hemorrhage patients: effects on regional cerebral blood flow," *Crit. Care Med.* **40**, 2797–2804 (2012).
43. B. Matta and D. Menon, "Severe head injury in the United Kingdom and Ireland: a survey of practice and implications for management," *Crit. Care Med.* **24**, 1743–1748 (1996).
44. H. Moseley et al., "Propofol: a new intravenous anaesthetic," *West Indian Med. J.* **37**, 229–231 (1988).
45. T. Kazama et al., "Relation between initial blood distribution volume and propofol induction dose requirement," *Anesthesiology* **94**, 205–210 (2001).
46. J. Selb et al., "Improved sensitivity to cerebral hemodynamics during brain activation with a time-gated optical system: analytical model and experimental validation," *J. Biomed. Opt.* **10**, 011013 (2005).
47. T. R. Garski et al., "Adverse reactions after administration of indocyanine green," *J. Am. Med. Assoc.* **240**, 635 (1978).
48. M. Diop and K. St Lawrence, "Improving the depth sensitivity of time-resolved measurements by extracting the distribution of times-of-flight," *Biomed. Opt. Express* **4**, 447–459 (2013).
49. S. Strebel et al., "Dynamic and static cerebral autoregulation during isoflurane, desflurane, and propofol anesthesia," *Anesthesiology* **83**, 66–76 (1995).
50. K. H. Polderman, "Application of therapeutic hypothermia in the intensive care unit. Opportunities and pitfalls of a promising treatment modality—Part 2: practical aspects and side effects," *Intensive Care Med.* **30**, 757–769 (2004).
51. K. H. Polderman, "Mechanisms of action, physiological effects, and complications of hypothermia," *Crit. Care Med.* **37**, S186–S202 (2009).
52. J. van der Linden et al., "Is cerebral blood flow/metabolic mismatch during rewarming a risk factor after profound hypothermic procedures in small children?," *Eur. J. Cardiothorac. Surg.* **3**, 209–215 (1989).
53. T. Shiozaki et al., "Effect of mild hypothermia on uncontrollable intracranial hypertension after severe head injury," *J. Neurosurg.* **79**, 363–368 (1993).
54. J. T. Povlishock and E. P. Wei, "Posthypothermic rewarming considerations following traumatic brain injury," *J. Neurotrauma* **26**, 333–340 (2009).

Mohammad Fazel Bakhsheshi received his PhD in medical biophysics from Western University, Canada, in 2014. He received his BSc degree in mechanical engineering from the University of Tehran, Iran, and MSc degree in mechanical engineering from Western University, Canada. He is currently a postdoctoral researcher at Robarts Research Institute. His research interests include application of optics in brain temperature monitoring and developing of selective brain cooling methods to induce hypothermia.

Mamadou Diop obtained a PhD in physics from the Center for Optics, Photonics, and Lasers at Laval University (Quebec). He then took a two-year postdoctoral position at the Institute for Microsctructural Sciences of the National Research Council (NRC) of Canada in Ottawa. After completion of his postdoc, he moved to London (Ontario) to become a research associate at the Lawson Health Research Institute (LHRI). He is currently a research scientist with the imaging program of the LHRI at St. Joseph's Hospital, where he develops noninvasive optical instruments and algorithms for medical applications.

Laura B. Morrison received an associate degree in veterinary technology from the University of Guelph (Ridgetown) and became a registered veterinary technician in 2005. She graduated from the University of Guelph in 2008 with a Bachelor of Science in animal science. She started working in imaging research at Lawson Health Research Institute in 2010 and acquired registered laboratory animal technician status through the Canadian Association for Laboratory Animal Science in 2012. She continues to work passionately with many biomedical imaging research projects and has been a previously published co-author.

Keith St. Lawrence is an associate professor in medical biophysics at the University of Western Ontario and a scientist at the LHRI. His research focuses on the development and application of imaging modalities, including optical methods, for mapping brain function and assessing cerebrovascular health. He is currently supported by a personnel award from the Heart and Stroke Foundation, Ontario Provincial Office, to develop optical techniques for detecting cerebral ischemia in critical-care patients.

Ting-Yim Lee is director of PET/CT imaging research at Lawson Health Research Institute, a scientist with Robarts Research Institute, and a professor of medical imaging at the University of Western Ontario. His research focuses on the use of imaging to study physiological processes in diseases. His lab has pioneered a method of using x-ray dye and CT scanning to measure blood flow in various tissues, including the brain, tumors, and the heart.